

The effect of halofuginone on radiation-induced cardiovascular injury

Cagdas Yavas¹, Mustafa Calik², Guler Yavas³, Hatice Toy⁴, Hidir Esme²,
Goknil Calik⁵, Mustafa Fevzi Sargon⁶

¹Department of Radiation Oncology, Konya Training and Research Hospital, Konya, Turkey

²Department of Thoracic Surgery, Konya Training and Research Hospital, Konya, Turkey

³Department Radiation Oncology, Selcuk University, Faculty of Medicine, Konya, Turkey

⁴Department of Pathology, Necmettin Erbakan University, Meram Faculty of Medicine, Konya, Turkey

⁵Department of Emergency Medicine, Necmettin Erbakan University, Meram Faculty of Medicine, Konya, Turkey

⁶Department of Anatomy, Hacettepe University, Faculty of Medicine, Ankara, Turkey

Received January 12, 2015; Revised February 10, 2015; Accepted February 13, 2015; Published Online February 26, 2015

Original Article

Abstract

Purpose: The main purpose of this study was to evaluate the effects of Halofuginone on radiation-induced cardiovascular injury in a rat model. **Methods:** Sixty Wistar-Albino rats were divided into six groups (the control group, radiotherapy (RT) only group Irradiation (IR), 2.5 and 5 µg Halofuginone groups (Hal (2.5)/C and Hal (5.0)/C), and RT plus 2.5 and 5 µg Halofuginone groups (Hal (2.5)/IR and Hal (5.0)/IR). Rats were exposed to a single dose of 12 Gy irradiation generated by a linear accelerator. Halofuginone was applied intraperitoneally with daily doses. At the 6th and 16th weeks of RT, 5 rats from each group sacrificed and; heart and thoracic aorta tissues removed for both light microscopic and electron microscopic examinations. **Results:** Light microscopic examinations revealed that the endocardial thickness of all study groups was significantly different at 6th and 16th week of RT ($p < 0.001$ for both). Pair-wise comparisons showed that the differences were significant in IR- Hal (2.5)/IR ($p < 0.001$); IR-Hal (5.0)/IR ($p < 0.001$); and Hal (2.5)/IR-Hal (5.0)/IR ($p = 0.001$) at 16th week of RT. There were significant differences within the study groups regarding to the thoracic aorta fibrosis scores only at 16th week of RT ($p = 0.002$). Electron microscopic examinations demonstrated that there were significant differences between all the groups with respect to heart mitochondria scores at both 6th week and 16th weeks of RT ($p < 0.001$ for both). The differences between Hal (2.5)/IR and Hal (5.0)/IR with respect to the heart mitochondria scores were significant only at 16th week of RT ($p = 0.001$). **Conclusion:** These data demonstrated that Halofuginone may improve radiation-induced cardiovascular injury. The most prominent improvement was observed in higher dose of Halofuginone group after long term follow-up.

Keywords: Halofuginone; Cardiovascular Toxicity; Radiotherapy; Rat

Introduction

Cardiovascular disease and cancer are the two leading causes of morbidity and mortality worldwide.¹ The majority of the radiation-induced cardiovascular disease has been reported in patients who previously treated with thoracic irradiation for Hodgkin's disease and breast cancer. Estimated relative risk of fatal cardiovascular events after irradiation for Hodgkin's disease and left-sided breast cancer range between 2.2 and 7.2 and 1.0 to 2.2, respectively.² Risk is life long, and absolute risk appears to increase with length of time since exposure. Radiation-associated cardiovascular toxicity may in fact be progressive.³

Primary basic mechanisms behind radiation-induced cardiovascular disease appear to be endothelial dysfunction.⁴⁻⁶ The sequence of endothelial injury, cell detachment, thrombosis

and fibrosis results in significant tissue injury that often limits radiation oncologist in attempting to deliver curative doses to a nearby tumor. Fajardo and Steward have demonstrated that damage to the myocardium develops through three phases of injury.⁵ During acute phase a neutrophilic infiltrate develops involving all layers of the heart and vessels. The latent phase is notable for remarkably healthy pericardium and myocardium, which shows only slight, progressive fibrosis. Myocardial capillary endothelial cells demonstrate progressive damage leading to obstruction of the lumen and thrombi of fibrin and platelets. Though healthy endothelial cell replication in the vicinity occurred, it is generally inadequate and an inevitable ischemia leads to progressive fibrosis. Animals begin to die at approximately 70th day due to extensive fibrosis. The hallmark of this late stage is extensive fibrosis.²

Corresponding author: Cagdas Yavas; Department of Radiation Oncology, Konya Training and Research Hospital, Konya, Turkey.

Cite this article as: Yavas C, Calik M, Yavas G, Toy H, Esme H, Calik G, Sargon MF. The effect of halofuginone on radiation-induced cardiovascular injury. *Int J Cancer Ther Oncol* 2015; 3(2):03029. DOI: 10.14319/ijcto.0302.9

[A part of this research was presented as an "Oral presentation" at MASCC/ISOO-2013, Annual Meeting, which was held from June 27-29, 2013 in Berlin, Germany]

Halofuginone is a, low molecular weight plant derived alkaloid, isolated from the *Dichroa febrifuga* plant that exhibits antifibrotic activity and inhibition of type I collagen synthesis.⁷ As fibrosis is the result of an increase in type I collagen, it is assumed that selective inhibition of type I collagen synthesis may inhibit formation of fibrosis without affecting tissue structure.⁸ To the best of our knowledge there is no study in the literature observing the effect of Halofuginone on the radiation-induced cardiovascular injury. The present study was designed to determine whether Halofuginone treatment would ameliorate the radiation-induced cardiovascular injury.

Methods and Materials

Study design

The study included 60 adult female Wistar-Albino rats (250-300 g), the use of which was approved by the Necmettin Erbakan University Animal Care and Use Committee. Animals were housed 4 per cage in a controlled animal holding room with a 12/12-h light/dark cycle; temperature and relative humidity were continually monitored to provide standard laboratory conditions. Food and water were provided ad libitum. The rats were randomly grouped into four groups containing 10 rats each: In control group (Control), neither radiotherapy (RT) nor medication administered.

IR was the RT only group receiving a single dose of RT (12 Gy), but no medication. Hal (2.5)/C and Hal (5.0)/C were 2.5 µg and 5 µg Halofuginone groups and rats in these groups were applied Halofuginone (Collgard Biopharmaceuticals Ltd. Petah Tikva, Israel) in a single dose of 2.5 µg and 5 µg daily intraperitoneal injection for 16 weeks respectively. Hal (2.5)/IR and Hal (5.0)/IR were defined as 2.5 µg Halofuginone + RT and 5 µg Halofuginone + RT groups and rats in these groups were given Halofuginone in a single dose of 2.5µg and 5 µg daily intraperitoneal injections for 16 weeks, starting immediately after administration of 12 Gy single dose radiotherapy.

Irradiation protocol

RT was applied under general anesthesia with intraperitoneally administered 90 mg/kg ketamine hydrochloride and 10 mg/kg xylazine. A single dose of 12 Gy with 6 MV photon beams was applied via a single anterior field to 2 cm depth with SAD (source-axis distance) technique. 1 cm elasto-gel bolus was used to build up the radiation dose on the heart and to provide contour regularity. The field size was 4 × 4 cm and included the mediastinum.

Halofuginone protocol

Halofuginone is in crystalline form. Crystalline Halofuginone was dissolved in a 0.44 M, pH 4.3 lactic acid tampons and stock solutions of 1-2 mg/ml were prepared and stored at 4°C at which it could remain stable for at least 4 months. Study

solutions for injection were prepared by diluting the stock solutions daily using 0.9% NaCl (0.1 mg/1 ml). The study solutions were used within 1 hour following preparation.

Morphologic studies

At the 6th and 16th weeks of the RT, five animals from each group were anesthetized and sacrificed by cervical dislocation. The heart and thoracic aorta removed from the chests of the animals.

Light microscopy

The heart and thoracic aorta samples were excised and fixed in 10% formaldehyde solution and embedded in paraffin for light microscopic examination. The slices obtained were stained with hematoxylen and eosin (H&E) to evaluate the inflammation, and with immunohistochemical triple staining to identify the cardiac fibrosis. As a quantitative end point, extend of the radiation-induced fibrosis, was graded on a scale of 0 (normal heart-normal aorta) to 3 (severe fibrosis) as described in **Table 1**.

Using the digital images obtained from the selected areas by light microscopy (Nikon, Labophot-2, Japan) at magnification x20, the thickness of the endocardium was measured by BAB system (BAB Bs200Pro Image Analysis Software, BAB Yazılım Donanım Mühendislik Medikal San.Ve Tic. Ltd. Sti. Ankara, Turkey). The pathologist was not aware of the treatment groups at the time of the histological examination of the specimens. After examining the whole sections for each rat, the average value was taken as the fibrosis score and mean values of the groups were calculated.

TABLE 1: The scoring system for fibrosis of the heart and thoracic aorta samples with light microscopy.

Score	Fibrosis
0	Normal
1	Minimal
2	Moderate
3	Severe

Electron microscopy

The tissue samples which were taken from the animals 6 and 16 weeks after RT were put into 2.5% glutaraldehyde for 24 hours for primary fixation. The same application was done to the rats of the Halofuginone and control groups after the administration of the drug or NaCl in the same timing procedure. Then, these samples were washed with Sorenson's Phosphate Buffer solution (pH: 7.4) and they were post-fixed in 1% osmium tetroxide. After post-fixation, they were washed with the same buffer and dehydrated in increasing concentrations of alcohol series. After dehydration, the tissues were washed with propylene oxide and embedded in epoxy resin embedding media. The semi-thin and ultrathin sections of the obtained tissue blocks were cut with an ultramicrotome (LKB Nova, Sweden). These semi-thin sections which were 2 micrometers in thickness were stained with

methylene blue and examined under a light microscope (Nikon, Japan). Following this procedure, trimming was done to the tissue blocks and their ultrathin sections which were about 60 nanometers in thickness were taken by the same ultramicrotome. These ultra-thin sections were stained with uranyl acetate and lead citrate and they were examined under Jeol JEM 1200 EX (Japan) transmission electron microscope. The electron micrographs of the specimens were taken by the same microscope.

The parameters which were investigated by electron microscopy regarding to thoracic aorta samples for each rat were endothelial cells, subendothelial layer, and internal elastic membrane, smooth muscle cells of the tunica media, external elastic membrane and collagen fibers and fibroblasts of tunica externa (adventitia). Since the only morphological appearance of endothelial cells and the severity of subendothelial edema were different among groups, a scoring system which was defined in our previous study was performed based on these 2 parameters which was listed in **Table 2**.⁹

TABLE 2: The scoring system for the damage signs of vascular injury for electron microscopy.

Score	Endothelial Cells	Subendothelial Edema
0	Normal	No edema
1	Slight thinning	Minimal edema
2	Apparent thinning	Intensive edema
3	Detachment from basement membrane	
4	Detachment from basement membrane and apparent thinning	

In order to define cardiac injury, mitochondrial samples were examined using a scoring system (**Table 3**). In each group; mitochondria were scored in five samples. For every sample; 100 mitochondria were scored; therefore for each group; totally 500 mitochondria were scored.

TABLE 3: The scoring system for cardiac mitochondria.

Score	Mitochondria Score
0	Ultrastructurally normal
1	Mitochondrion with prominent cristae
2	Swollen mitochondrion (cloudy swelling)
3	Amorphous material collection in mitochondrion

Statistical method

The Statistical Package for Social Sciences (SPSS) v. 16.0 was used for statistical analyses. As the pathological scores were ordinal in nature, the differences in pathological findings

between the study groups were analyzed using the Kruskal-Wallis test. When an overall statistically significant difference was observed, pair-wise comparisons were performed using the Mann-Whitney U test. Bonferroni correction was used for multiple comparisons. A 5% type-I error level was used for the statistical significance cut-off for overall comparisons.

Results

Pathological changes of the heart and the thoracic aorta samples six weeks after radiotherapy are presented below.

Light microscopy

Thoracic aorta samples

Histopathological examinations of the thoracic aorta samples revealed a subendothelial edema in the IR group. Moreover there was a severe inflammation in the tunica adventitia in this group. However the amount of the subendothelial edema and inflammation were not severe in Hal (2.5)/IR and Hal (5.0)/IR groups. There was not any ultrastructural change in the thoracic aorta samples of the control group, Hal (2.5)/C and Hal (5.0)/C groups. When the thoracic aorta fibrosis scores were compared, there were significant difference between the study groups ($p = 0.087$). Triple staining revealed minimal fibrosis in all the RT groups.

Heart samples

There weren't any ultrastructural changes in the heart samples of the control group, Hal (2.5)/C and Hal (5.0)/C groups. Hematoxylen-eosin (H&E) staining did not demonstrate any pathological findings in IR group except for the minimal moderate endothelial thickening. Similarly there were minimal thickening in the endocardium of the Hal (2.5)/IR and Hal (5.0)/IR groups. However the endocardial thickening of Hal (2.5)/IR and Hal (5.9)/IR groups were not as severe as IR group. Triple staining revealed subendocardial fibrosis in the IR, Hal (2.5)/IR and Hal (5.0)/IR groups.

Table 4 shows the endocardial thickness scores of the study groups. There was significant difference between the study groups with respect to the endocardial thickness scores at 6th week of RT ($p < 0.001$). The endocardial thickness score of the IR was significantly higher than Hal (2.5)/IR and Hal (5.0)/IR scores (p values were <0.001 for both). Also there was a significant difference between Hal (2.5)/IR and Hal (5.0)/IR in terms of the endocardial thickness scores ($p < 0.001$). There weren't any significant differences in control and Hal (2.5)/C ($p = 0.393$); IR and Hal (5.0)/C ($p = 0.739$) and; Hal (2.5)/C and Hal (5.0)/C ($p = 0.165$).

TABLE 4: Endocardial thickness values of each study group at 6th weeks and 16th weeks of RT.

	Mean	Standard Deviation	Median	Minimum	Maximum	p
6th week of RT						
Control	19,48	4,33	18,06	15,01	28,23	
IR	616,04	70,1	582,6	532,06	718,65	
Hal (2.5)/C	21,84	4,98	22,02	16,09	28,03	
Hal (5.0)/C	18,34	3,21	18,02	15,06	26,03	<0.001
Hal (2.5)/IR	466,87	28,55	468,05	412,2	505,13	
Hal (5.0)/IR	86,75	24,08	80,67	62,01	148,18	
16th week of RT						
Control	19,34	3,4	18,01	16,02	25,68	
IR	737,8	78,2	736,02	605,12	845,03	
Hal (2.5)/C	21,33	4,66	20,33	15,66	29,02	<0.001
Hal (5.0)/C	18,45	3,27	18,05	16,05	25,06	
Hal (2.5)/IR	99,81	1,32	98,75	77,42	121,03	
Hal (5.0)/IR	59,38	1,03	57,02	45,00	78,12	

We found statistically significant differences in endocardial thickness between the study groups at 6th weeks and 16th weeks of RT ($p < 0.001$, Kruskal-Wallis). The maximum endocardial thickening was observed in IR at 16th weeks of RT.

Electron microscopy

Thoracic aorta samples

There was a severe subendothelial edema in all the RT groups. However there wasn't any ultrastructural change in the thoracic aorta samples of the control group, Hal (2.5)/C and Hal (5.0)/C groups. Subendothelial vacuoles were present in the endothelial cells of H (2.5)/IR group. Additionally there was a severe subendothelial edema in this group. The ultrastructural finding of Hal (5.0)/IR group was same with IR group. When the subendothelial edema and the endothelial cell scores were compared at 6th week of RT, there were significant differences between all the groups (p values were < 0.001 for both parameters). Pair-wise comparisons of RT groups demonstrated that there were significant differences between IR and Hal (2.5)/IR, IR and Hal (5.0)/IR regarding to subendothelial edema scores; whereas there wasn't any difference between endothelial cell scores (p values were IR-Hal (2.5)/IR < 0.001 and 0.280 and IR-Hal (5.0)/IR 0.002 and 0.280 for subendothelial edema and endothelial cell scores respectively). On the other hand there wasn't any difference in terms of subendothelial edema and endothelial cell scores between Hal (2.5)/IR and Hal (5.0)/IR (p values were 0.739 and > 0.99 for subendothelial edema and endothelial cell scores respectively)

Heart samples

There weren't any ultrastructural changes in the heart samples of the Hal (2.5)/C and Hal (5.0)/C groups. The ultrastructural findings of both Halofuginone groups were same with control group. Histological examinations of the heart sections revealed that separations in the myofibrils were increased and the amount of glycogen was decreased in all of the RT groups. Most of the mitochondria were swollen. The perinuclear cisternae of the heart muscle cells were dilated severely. The ultrastructural appearance of the intercalated discs was damaged. In Hal (2.5)/IR group there were also swollen mitochondria. The amount of the swollen mitochondria was the least in Hal (5.0)/IR group. In this group also

the ultrastructural appearance of the intercalated discs was damaged.

TABLE 5: The mean of the cardiac mitochondria scores of the study groups with electron microscopy.

Group	6 th week of RT	16 th week of RT	p
Control	8.0±0.6	8.5±1.5	
IR	148.3±3.1	160.3±5.7	$p < 0.001$
Hal (2.5)/C	8.2±2.1	8.9±1.3	
Hal (5.0)/C	8.2±1.6	9.1±2.3	
Hal(2.5)/IR	117.7±3.9	112.5±5.8	
Hal(5.0)/IR	110.5±2.7	93.2±3.9	

Kruskal-Wallis test demonstrated that there was a significant difference between all the groups with respect to heart mitochondria scores at 6th week of RT ($p < 0.001$) (Table 5). When all the RT groups compared in terms of the mitochondria scores at 6th week of RT the differences between IR-Hal (2.5)/IR and IR- Hal (5.0)/IR were statistically significant (p values were < 0.001 for each).

The pathological changes of the heart and the thoracic aorta samples sixteen weeks after radiotherapy are presented below.

Light microscopy

Thoracic aorta samples

The histopathological findings of IR group were same with 6th week findings. However there weren't any changes in the samples taken from the control group, Hal (2.5)/C and Hal (5.0)/C; and Hal (2.5)/IR and Hal (5.0)/IR groups with H&E staining.

Kruskal-Wallis test revealed that there were significant differences within the study groups in terms of thoracic aorta fibrosis scores ($p = 0.002$). There weren't any changes in non-RT groups. However; Mann-Whitney U test demonstrated that there were significant differences between

IR-Hal (2.5)/IR, IR-Hal (5.0)/IR ($p = 0.007$ and $p = 0.002$, respectively).

Heart samples

H&E staining revealed extensive thickening in the endocardium in IR group. On the other hand minimal endocardial thickening was observed in Hal (2.5) IR and Hal (5.0)/IR groups. Also, Trippl staining confirmed a severe subendocardial fibrosis in IR group. However there were minimal subendocardial fibrosis in the Hal (2.5) IR and Hal (5.0)/IR groups (**Figure 5**).

There was a significant difference within the endocardial thickness of all study groups at 16th week of RT (**Table 4**) ($p < 0.001$). The maximum thickness was observed in IR. Pair-wise comparisons showed that there were significant differences between IR and Hal (2.5)/IR ($p < 0.001$); IR and Hal (5.0)/IR ($p < 0.001$) and; Hal (2.5)/IR and Hal (5.0)/IR ($p = 0.001$) regarding to endocardial thickness at 16th week of RT.

Electron microscopy

Thoracic aorta samples

There weren't any ultrastructural changes in the thoracic aorta samples of the control group, Hal (2.5)/C and Hal (5.0)/C groups. On the other hand there were severe subendothelial edema, separations and interruptions in the endothelium all RT groups. The ultrastructural findings of all RT groups were similar with respect to the thoracic aorta samples. When we compared all the groups regarding to the subendothelial edema and the endothelial cell scores at 16th week of RT, there were significant differences between all the groups (p values were < 0.001 for both parameters).

At 16th week of RT, there were significant differences only in between IR-Hal (2.5)/IR and IR-Hal (5.0)/IR in terms of endothelial cell scores (p values were IR-Hal (2.5)/IR < 0.001 and IR-Hal (5.0)/IR = 0.003). On the other hand subendothelial edema scores were not different for all the RT groups (p values were > 0.99 for each).

Heart samples

There were no ultrastructural changes in the heart samples of the control, Hal (2.5)/C and Hal (5.0)/C groups (**Figure 1, 2**). The same ultrastructural findings were observed in IR group when compared with 6th week's findings. The perinuclear cisternae of the heart muscle cells were dilated severely. The ultrastructural appearance of the intercalated discs was damaged. Amount of swollen mitochondria was increased. Additionally fibrosis was observed in between the myofibrils (**Figure 3**). Also the findings of Hal (2.5)/IR group were same with 6th week findings. In Hal (5.0)/IR group the mitochondria score was better than the previous heart samples (**Figure 4**). The separations in myofibrils were less than that of previous Hal (5.0)/IR group.

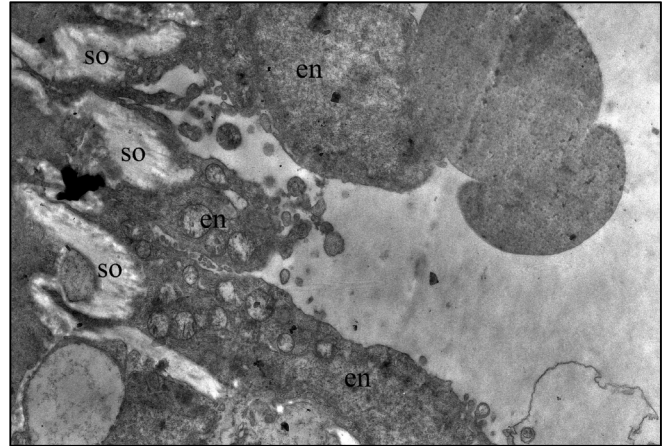


FIG. 1 (Heart sample of Control group at 16th week): Electron micrograph showing normal cardiac structure (Original magnification X7500).

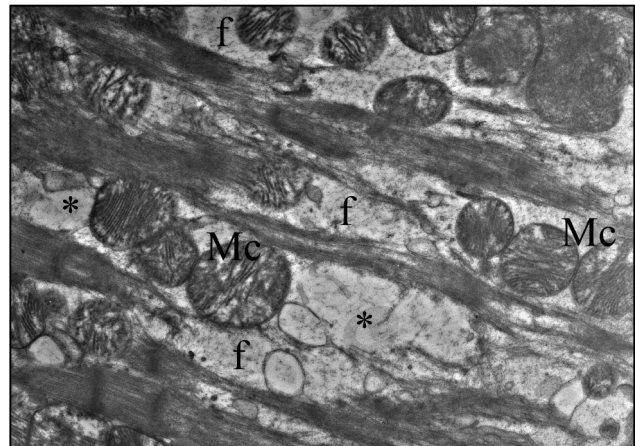


FIG. 2 (Heart sample of Hal (5.0)/ C group at 16th week): Electron micrograph showing ultrastructurally normal heart muscle (n = nucleus of heart muscle cell; m = ultrastructurally normal mitochondria) (Original magnification X7500).

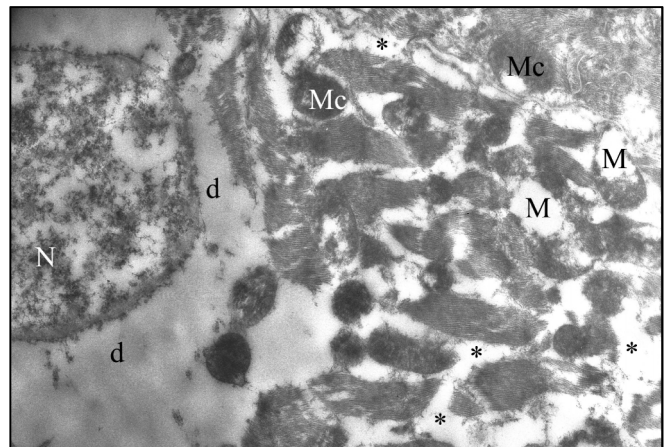


FIG. 3 (Heart sample of IR group at 16th week): Electron micrograph showing separations in myofibrils (*), mitochondria with prominent cristae (Mc) and fibrosis (f) (Original magnification X7500).

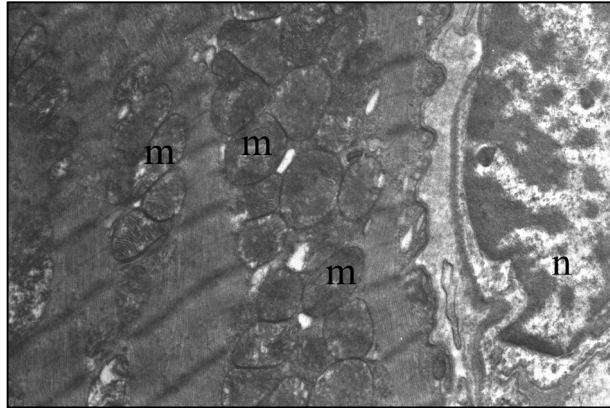


FIG. 4 (Heart sample of Hal (5.0)/IR group at 16th week): Electron micrograph showing mitochondria with prominent cristae (Mc). Most of the mitochondria's were swollen. The ultrastructural appearance of intercalated discs were damaged (N = nucleus; Mc = mitochondrial cristae; M = mitochondria; d = discus intercalaris) (Original magnification X7500).

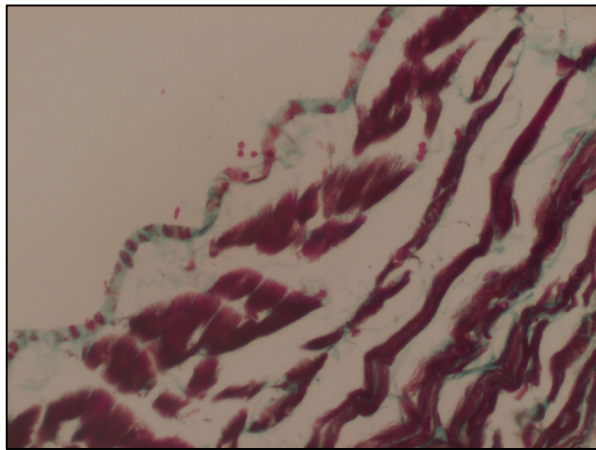


FIG. 5a (Heart sample of Control group at 16th, Tripplle staining): Normal cardiac structure (X200)

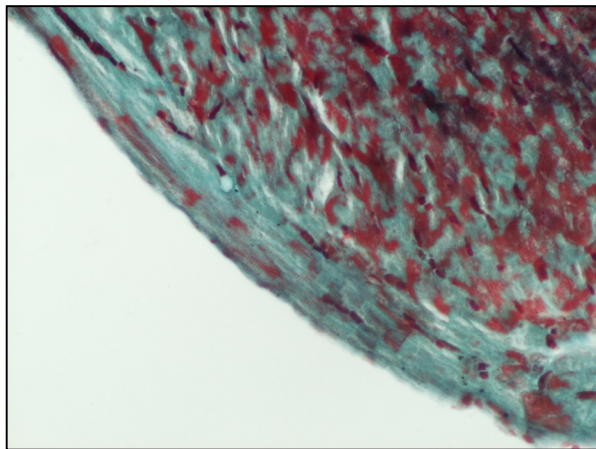


FIG. 5b (Heart sample of IR group at 16th, Tripplle staining): There was extensive subendocardial fibrosis (X200)

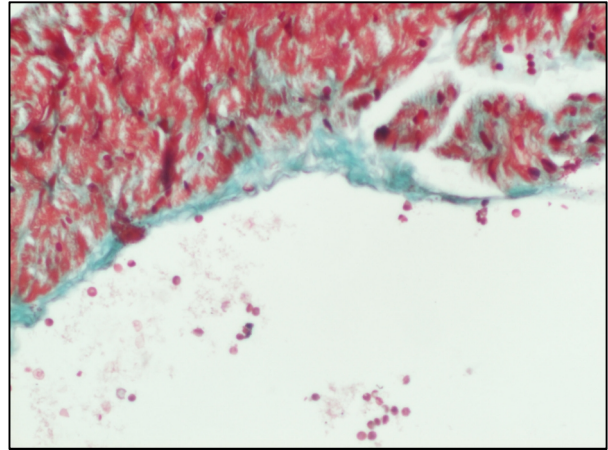


FIG. 5c (Heart sample of Hal (2.5)/IR group at 16th week, Tripplle staining): There was minimal subendocardial fibrosis (X200).

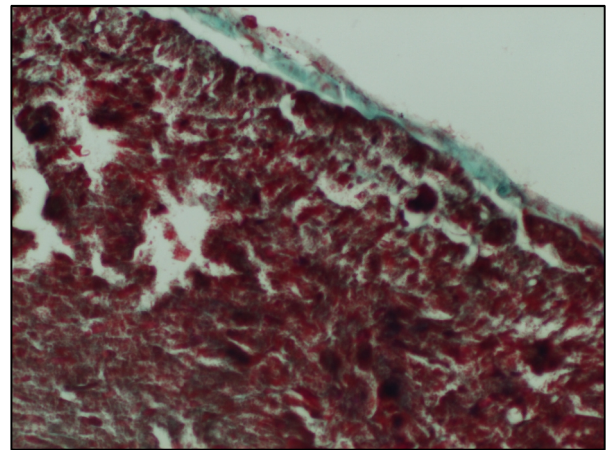


FIG. 5d (Heart sample of Hal (5.0)/IR group at 16th week, Tripplle staining): There was minimal subendocardial fibrosis. (X200)

When the heart mitochondria scores were compared at 16th week of RT, there were significant differences between all the groups ($p < 0.001$) (Table 5). Mann-Whitney U test demonstrated that there were significant differences between IR-Hal (2.5)/IR, IR-Hal(5.0)/IR and Hal (2.5)/IR-Hal (5.0)/IR in terms of mitochondria scores (p values were <0.001 for IR-Hal (2.5)/IR and IR-Hal (5.0)/IR; and $= 0.001$ for Hal (2.5)/IR-Hal (5.0)/IR).

Discussion

Although the heart was initially thought to be relatively resistant to radiation-induced injury, cardiovascular diseases resulting from therapeutic irradiation is now well recognized.¹⁻³ The worldwide number of long-term cancer survivors has been growing in parallel to the improvements in cancer therapies. However, long-term survivors may suffer from late side effects of RT. One of these side effects is radiation-induced cardiovascular disease which may occur in patients who previously treated with thoracic irradiation for Hodgkin's disease and breast cancer.

Numerous studies of radiation-induced toxicity show that “endothelial cell injury” is the key point in most tissues, even though the endothelial cells comprise only a minor fraction of cardiac cells.^{4, 10, 11} The sequence of endothelial injury, cell detachment, thrombosis and fibrosis results in significant tissue injury that often limits radiation oncologist in attempting to deliver curative doses to a nearby tumor. The hallmark of radiation-induced injury is extensive fibrosis. The fibrotic phase tends to manifest >3 months RT. Fibrosis is a kind of wound healing process. Transforming growth factor β -1 (TGF- β 1) plays an integral role in fibrosis formation by promoting the chemoattraction of fibroblasts and their conversion to myofibroblasts.¹²

Halofuginone, (7-bromo-6-chloro-3-[3-(3-hydroxy-2-piperidinyl)-2-oxopropyl]-4(3H)-quinazolinone) an alkaloid isolated from the *Dichroa febrifuga* plant, originally used in fowl as an anticoccidiostatic food supplement, reduces avian skin collagen content. In vitro, treating cultured dermal fibroblasts with Halofuginone attenuates the incorporation of proline into collagenase digestible proteins, without affecting the production of non-collagenase digestible proteins, cell proliferation, or collagen degradation. Halofuginone specifically inhibits collagen α 1 gene expression, resulted in a decrease in collagen synthesis, and the TGF- β induced collagen synthesis.^{8, 13, 14}

It has been demonstrated that Halofuginone reduces fibrosis formation in many pathological conditions.^{8, 13-19} Previously Halofuginone has shown to reduce fibrosis in mice models with stretched skin due to scleroderma²⁰, to decrease in the liver fibrosis model due to thiocetamide²¹, to lessen graft versus host disease²², to improve muscular dystrophies including dysferlinopathy^{19, 23}, and lessen mesangial cell proliferation and matrix deposition in the kidney.²⁴ By the light of these studies, we hypothesized that Halofuginone may be able to ameliorate radiation-induced cardiovascular injury. Our results suggested the Halofuginone improves radiation-induced cardiovascular injury. The most prominent improvement was observed in higher dose of Halofuginone and after long term follow-up in the heart samples.

Ertugrul and colleagues²⁵ administered intraperitoneal Halofuginone for 30 days to a group of rats after they traumatized the subglottic area, while they monitored the second group as controls. In the histopathological examinations of the subglottic areas, they found that fibrosis formation was significantly less in rats treated with Halofuginone when compared to that of control group. Ozelik and colleagues²⁶ administered intraperitoneal Halofuginone for 21 days after producing corrosive substance injury in the rat esophagus using 50% NaOH. They performed a histopathological examination and measured

the hydroxyproline levels of esophageal tissue of rats killed on day 21 in order to assess the fibrosis and stenosis index. Hydroxyproline levels and stricture formation in the Halofuginone group were found to be significantly lower than that of the control group. Moreover Dabak and colleagues²⁷ observed the effect of Halofuginone on preventing esophageal and hypopharyngeal fibrosis and suggested that Halofuginone can be used safely to prevent radiation-induced esophageal and hypopharyngeal fibrosis.

Xavier and colleagues suggested new ideas on the molecular mechanisms of the inhibition of TGF- β 1 signal production with Halofuginone, and demonstrated that Halofuginone reduces the radiation-induced leg contraction in mice.⁸ Therefore the authors conducted a new study to determine if less dosing of Halofuginone would result in protection against leg contracture.¹⁷ In this study authors used five daily doses of Halofuginone (instead of seven) per week during 4 months of period. They demonstrated that, Halofuginone is a protector against radiation-induced leg contraction (fibrosis) by attenuating the induction of key members of the TGF- β signaling pathway. The authors also showed that Halofuginone did not protect against radiation-induced tumor re-growth delay. Therefore the authors conducted a new study to determine if Halofuginone might enhance the radiosensitivity of human tumor cell lines.²⁸ Their study revealed that Halofuginone treatment inhibited cell growth, halted cell cycle progression, decreased radiation-induced DNA damage repair and decreased TGF- β receptor II protein levels, leading to increased cellular radiosensitization.

In the current study we compared two different doses of Halofuginone. Different from the study by Ishii and colleagues, we applied the Halofuginone during whole week including the weekends. Our results suggested that using 5 μ g Halofuginone resulted in more prominent improvement. This finding was observed at 6th week of RT as well as 16th week of RT. When we compared the 2.5 μ g Halofuginone+RT and 5 μ g Halofuginone+RT groups at 16th week of RT, we found a significant difference between two groups with respect to endocardial thickness scores. On the other hand at 6th week of RT we could not demonstrate any significant differences between thoracic aorta samples of the RT groups. However, at 16th week of RT electron microscopy revealed that endothelial damage was more prominent in RT only group when compared to that of RT+Halofuginone groups. In the same manner light microscopy revealed that at 16th week of RT there were severe fibrosis in the thoracic aorta samples of RT only group however this finding was not observed in RT+Halofuginone groups.

In a current study investigating the effects of concomitant RT and Trastuzumab on vascular structures two different

doses of RT were compared: 8 Gy and 15 Gy.⁹ The 8 Gy dose of RT was not enough to cause significant changes both from functional and morphological aspects. On the other hand 15 Gy RT led significant changes. In the current study we used a RT dose between these two doses. Our results suggested that 12 Gy RT seems to be enough in order to observe radiation-induced cardiovascular toxicity in rat studies.

Conclusion

The current study is the first one observing the effect of Halofuginone on radiation-induced cardiovascular injury. Our results suggested that the use of Halofuginone improves radiation-induced injury on the heart as well as the thoracic aorta. The effect was more prominent in the heart samples when compared to the thoracic aorta samples, at higher dose and after long term follow-up. This finding should be clarified with further clinical studies.

Conflict of interest

The authors declare that they have no conflicts of interest. The authors alone are responsible for the content and writing of the paper.

Acknowledgement

This work is supported by supported by Konya Training and Research Hospital. There is no role of study sponsors in the study design, in the collection, analysis and interpretation of data; in the writing of the manuscript and in the decision to submit the manuscript for publication. We did not have a financial relationship with the organization that sponsored the research.

References

1. Fuster V, Voûte J. MDGs: chronic diseases are not on the agenda. *Lancet* 2005; **366**:1512-4.
2. Adams MJ, Hardenbergh PH, Constine SL, Liphultz SE. Radiation-associated cardiovascular disease. *Critical reviews in oncology/ Hematology* 2003; **45**: 55-75.
3. Curigliano G, Cardinale D, Suter T, et al. Cardiovascular toxicity induced by chemotherapy, targeted agents and radiotherapy: ESMO Clinical Practice Guidelines. *Ann Oncol* 2012; **23**: vii155-66.
4. Zidar N, Ferluga D, Hvala A, et al. Contribution to the pathogenesis of radiation-induced injury to large arteries. *J Laryngol Otol* 1997; **111**:988-90.
5. Stewart JR, Fajardo LF. Radiation-induced heart disease. Clinical and experimental aspects. *Radiol Clin North Am* 1971; **9**:511-31.
6. Stewart JR, Fajardo LF, Gillette SM, Constine LS. Radiation injury to the heart. *Int J Radiat Oncol Biol Phys* 1995; **31**:1205-11.
7. Dent P, Yacoub A, Contessa J, et al. Stress and radiation-induced activation of multiple intracellular signaling pathways. *Radiat Res* 2003; **159**:283-300.
8. Xavier S, Piek E, Fujii M, et al. Amelioration of radiation-induced fibrosis: inhibition of transforming growth factor-beta signaling by halofuginone. *J Biol Chem* 2004; **279**:15167-76.
9. Yavas G, Yildiz F, Guler S, et al. Concomitant trastuzumab with thoracic radiotherapy: a morphological and functional study. *Ann Oncol* 2011; **22**:1120-6.
10. Gold H. Production of arteriosclerosis in the rat. Effect of x-ray and a high-fat diet. *Arch Pathol* 196; **71**:268-73.
11. Lamberts HB, de Boer W. Contributions to the study of immediate and early x-ray reactions with regard to chemo-protection. VII. X-ray-induced atheromatous lesions in the arterial wall of hypercholesterolaemic rabbits. *Int J Radiat Biol* 1963; **6**:343-50.
12. Graves PR, Siddiqui F, Anscher MS, Movsas B. Radiation pulmonary toxicity: from mechanisms to management. *Semin Radiat Oncol* 2010; **20**:201-7.
13. Pines M, Nagler A. Halofuginone: a novel antifibrotic therapy. *Gen Pharmacol* 1998; **30**:445-50.
14. Nelson EF, Huang CW, Ewel JM, et al. Halofuginone down-regulates Smad3 expression and inhibits the TGFbeta-induced expression of fibrotic markers in human corneal fibroblasts. *Mol Vis* 2012; **18**:479-87.
15. Zeplin PH, Larena-Avellaneda A, Schmidt K. Surface modification of silicone breast implants by binding the antifibrotic drug halofuginone reduces capsular fibrosis. *Plast Reconstr Surg* 2010; **126**:266-74.
16. Zeplin PH. Reduction of burn scar formation by halofuginone-eluting silicone gel sheets: a controlled study on nude mice. *Ann Plast Surg* 2012; **68**:271-5.
17. Ishii H, Choudhuri R, Mathias A, et al. Halofuginone mediated protection against radiation-induced leg contracture. *Int J Oncol* 2009; **35**:315-9.
18. Krane LS, Gorbachinsky I, Sirintrapun J, et al. Halofuginone-coated urethral catheters prevent periurethral spongiofibrosis in a rat model of urethral injury. *J Endourol* 2011; **25**:107-12.
19. Halevy O, Genin O, Barzilai-Tutsch H, et al. Inhibition of muscle fibrosis and improvement of muscle histopathology in dysferlin knock-out mice treated with halofuginone. *Histol Histopathol* 2013; **28**:211-26.

20. McGaha TL, Phelps RG, Spiera H, Bona C. Halofuginone, an inhibitor of type-I collagen synthesis and skin sclerosis, blocks transforming-growth-factor-beta-mediated Smad3 activation in fibroblasts. *J Invest Dermatol* 2002; **118**:461-70.
21. Bruck R, Genina O, Aeed H, *et al.* Halofuginone to prevent and treat thioacetamide-induced liver fibrosis in rats. *Hepatology* 2001; **33**:379-86.
22. Pines M, Snyder D, Yarkoni S, Nagler A. Halofuginone to treat fibrosis in chronic graft-versus-host disease and scleroderma. *Biol Blood Marrow Transplant* 2003; **9**:417-25.
23. Pines M, Halevy O. Halofuginone and muscular dystrophy. *Histol Histopathol* 2011; **26**:135-46.
24. Nagler A, Katz A, Aingorn H, *et al.* Inhibition of glomerular mesangial cell proliferation and extracellular matrix deposition by halofuginone. *Kidney Int* 1997; **52**:1561-9.
25. Ertuğrul EE, Cincik H, Dogru S, *et al.* Effects of halofuginone on fibrosis formation secondary to experimentally induced subglottic trauma. *Laryngoscope* 2007; **117**:299-302.
26. Özçelik MF, Pekmezci S, Saribeyoğlu K, *et al.* The effect of halofuginone, a specific inhibitor of collagen type 1 synthesis, in the prevention of esophageal strictures related to caustic injury. *Am J Surg* 2004; **187**:257-60.
27. Dabak H, Karlidag T, Akpolat N, *et al.* The effects of methylprednisolone and halofuginone on preventing esophageal and hypopharyngeal fibrosis in delivered radiotherapy. *Eur Arch Otorhinolaryngol* 2010; **267**:1429-35.
28. Cook JA, Choudhuri R, Degraff W, *et al.* Halofuginone enhances the radiation sensitivity of human tumor cell lines. *Cancer Lett* 2010; **289**:119-26.